Brain Imaging and Behavior (2018) 13:270–282
https://doi.org/10.1007/s11682-018-9857-5

ORIGINAL RESEARCH

Altered effective connectivity anchored in the posterior cingulate cortex and the medial prefrontal cortex in cognitively intact elderly APOE ε4 carriers: a preliminary study

Xiao Luo[1] · Kaicheng Li[1] · Y. L. Jia[1] · Qingze Zeng[1] · Yeerfan Jiaerken[1] · Tiantian Qiu[1] · Peiyu Huang[1] · Xiaojun Xu[1] · Zhujing Shen[1] · Xiaojun Guan[1] · Jiong Zhou[2] · Chao Wang[1] · J. J. Xu[1] · Minming Zhang[1] · for the Alzheimer's Disease Neuroimaging Initiative (ADNI)

Published online: 17 March 2018

Abstract

The APOE ε4 allele is associated with impaired intrinsic functional connectivity in neural networks, especially in the default mode network (DMN). However, effective connectivity (EC) reflects the direct causal effects of one brain region to another, which has rarely been investigated. Recently, Granger causality analysis (GCA) proved suitable for the study of directionality in neuronal interactions. Using GCA, we examined the differences in the EC between the anterior medial prefrontal cortex/posterior cingulate cortex (aMPFC/PCC) and the whole brain in 17 ε4 carrying and 32 non-carrying cognitively intact elderly individuals. Furthermore, correlation analyses were performed between the abnormal EC and cognition/neuropathological indices. Compared with the non-carriers, the results showed that the ε4 carriers exhibited decreased EC from the PCC to the whole brain in the middle temporal gyrus (MTG), the anterior cingulate cortex (ACC), and the precuneus (PCu). Meanwhile, the ε4 carriers demonstrated increased EC from the whole brain to the aMPFC in the inferior parietal lobe (IPL) and the postcentral gyrus (PCG). The correlation analyses suggested that the EC from the IPL/PCG to the aMPFC was related to episodic memory in non-carriers, while the decreased EC from the PCC to the ACC was associated with increased levels of t-tau in the ε4 carriers. In ε4 carriers, a negative influence can be traced from the PCC to both the anterior and posterior DMN subsystems; meanwhile, the anterior DMN subsystem receives compensatory effects from the parietal cortex. Early increases in AD-related pathologies in the PCC may act as first factors during this pathological process.

Keywords Resting-state functional MRI · APOE · Granger causality analysis, Default mode network · Effective connectivity · Cerebrospinal fluid

Introduction

Alzheimer's disease (AD) is the most common form of dementia and is characterized by memory loss, with the possible complication of cognitive decline in other domains. The primary neuropathological alterations in AD involves extracellular β-amyloid deposits and intraneuronal neurofibrillary tangles. (Montine et al. 2016). Multiple risk factors influence the occurrence of AD. The apolipoprotein E (APOE, gene) allele is the most reliable genetic risk factor for developing sporadic AD, accounting for 40% of AD cases (Liu et al. 2013). APOE ε4 carriers have a quadrupled risk, compared to ε3 homozygotes, of developing AD. At the foundation of previous animal studies, the APOE ε4 allele is thought to confer AD risk via decreased efficiency to bind unphosphorylated tau and to clear amyloid deposition (Padayachee et al. 2016; Farfel et al. 2016). The well-established association between the APOE ε4 allele and AD suggests that studying brain abnormalities in healthy APOE ε4 carriers may facilitate the understanding of the neural circuitry of AD and lead to earlier diagnoses and clinical treatments.

Electronic supplementary material The online version of this article (https://doi.org/10.1007/s11682-018-9857-5) contains supplementary material, which is available to authorized users.

✉ Minming Zhang
zhangminming@zju.edu.cn

[1] Department of Radiology, The 2nd Affiliated Hospital of Zhejiang University School of Medicine, No.88 Jie-Fang Road, Shang-Cheng District, Hangzhou 310009, China

[2] Department of Neurology, The 2nd Affiliated Hospital of Zhejiang University School of Medicine, Hangzhou, China

As for the APOE ε4 allele, recent neuroimaging studies and our previous work have frequently reported that it was associated with extensive abnormal brain networks within the default mode network (DMN), even in cognitively intact middle-aged and elderly subjects. During memory-encoding tasks, the APOE ε4 allele was related to a reduction in task-induced deactivations in the DMN (Trachtenberg et al. 2012; Persson et al. 2008). Recently, resting-state functional MRI (rsfMRI) has been widely used to investigate functional brain differences in APOE ε4 carriers. Most of the studies have reported significant resting-state functional connectivity (RSFC) differences in the DMN compared to NC (Yuan et al. 2016; Luo et al. 2016a, b). Specifically, Yuan et al. observed that the APOE ε4 allele simultaneously mediates the anterior and posterior DMN subnetworks by using RSFC analyses. Based on the ADNI database, one study demonstrated whole-brain ROI connectivity strength and ROI-to-ROI functional network connectivity strength between different APOE genotype groups and reported that APOE ε4 disrupted the network properties, mostly in the DMN (Mckenna et al. 2015). By setting the posterior cingulate cortex (PCC) as a seed, another study demonstrated that ε4 carriers had decreased in-phase connectivity in regions of the posterior DMN (Machulda et al. 2011).

Although previous studies have reported that a disconnection of the DMN could be one of the gene-expression profiles that exist in APOE ε4 carriers, the directionality of the influence between separate DMN regions has yet to be explored. It is known that functional connectivity is defined as the temporal correlations between spatially remote neurophysiological events. However, it does not provide any directional information about these associations (Friston 2011). In contrast, effective connectivity (EC) reflects the direct causal effect of one brain region on another brain region, which can help detail the neuropathological mechanisms of the functional architecture (Zang et al. 2012; Zhou et al. 2011). The Granger causality analysis (GCA) provides a feasible method for achieving this, by identifying directed functional interactions from time series data. Specifically, the GCA originated from the field of economics to assess causal relationships between two time series of economic sciences, based on the vector autoregressive (VAR) models/Geweke's feedback model (Granger 1969; Geweke 1982). This idea has been applied for time-directed predictions between BOLD-fMRI time series to explore the causal effects among specific brain regions (Yang et al. 2017; Jiao et al. 2011). Recently, GCA of rsfMRI data has proven to be valuable in analyzing EC in patients with AD, mild cognitive impairment (MCI) and normal aging (Jiao et al. 2011; Yang et al. 2017; Miao et al. 2011). In addition, few studies have simultaneously assessed intrinsic brain networks and AD-related pathologies (e.g., level of β-amyloid$_{1-42}$, tau protein), which could help in understanding the pathophysiologic substrates of APOE-related effects on EC mapping. To cover these gaps, here, we sought to characterize the functional circuit of the DMN in cognitively intact elderly individuals carrying the APOE ε4 allele, by assessing AD-related EC and CSF biomarkers.

According to the hierarchical clustering analysis, the DMN can be further divided into two subsystems (Andrews-Hanna 2012). First, the anterior DMN subsystem uses the anterior MPFC (aMPFC) as a connected node (Raichle 2015). Second, the posterior subsystem, which includes the PCC and the bilateral IPL, is mainly involved in the recollection of prior experiences (Yuan et al. 2016). The aim of the current study was twofold: first, to evaluate altered directional connectivity patterns from and to the PCC/aMPFC during the resting state in cognitively intact APOE ε4 carriers by utilizing whole-brain voxelwise GC analysis; second, to explore whether abnormalities in EC are related to cognition and CSF biomarkers.

Materials and methods

Alzheimer's disease neuroimaging initiative

The dataset used in this study was obtained from the Alzheimer's disease Neuroimaging Initiative (ADNI) database (adni.loni.usc.edu). The ADNI was launched in 2003 by the National Institute on Aging (NIA), the National Institute of Biomedical Imaging and Bioengineering (NIBIB), the Food and Drug Administration (FDA), private pharmaceutical companies and non-profit organizations, as a $60 million, 5-year public–private partnership. The primary goal of ADNI has been to test whether serial magnetic resonance imaging (MRI), positron emission tomography (PET), other biological markers, and clinical and neuropsychological assessment can be combined to measure the progression of mild cognitive impairment (MCI) and early Alzheimer's disease (AD). Determination of sensitive and specific markers of very early AD progression is intended to aid researchers and clinicians in developing new treatments and monitor their effectiveness, as well as lessen the time and cost of clinical trials.

Study participants

This study was approved by the Institutional Review Boards of all of the participating institutions, and informed written consent was obtained from all participants at each site. At the time of analysis, individuals carrying at least one APOE ε4 allele (genotype ε4/ε4 and ε4/ε3) were classified as APOE ε4 carriers, while individuals with the genotype ε3/ε3 were classified as non-carriers (normal controls, NC). Individuals with the ε2 allele (including genotype ε2/ε2, ε2/ε3, and ε2/ε4) were excluded due to its possible protective effects (Suri et al. 2013). Using the ADNI GO and ADNI 2 databases, 52 right-handed cognitively intact healthy

participants, comprising 19 APOE ε4 carriers and 33 NC, who had undergone structural scans, rsfMRI scans, and neuropsychological evaluations, were identified. The study data were downloaded from the publicly available ADNI database before January 15, 2017. According to the ADNI protocol, to be classified as NC, the subject must have had an MMSE score between 24 and 30 (inclusive) and a clinical dementia rating (CDR) score of 0. The subjects were also required to meet distinctive cutoffs for the Wechsler Memory Scale-Logical Memory (WMS-LM) delay score (in detail: ≥ 9 for subjects with 16 or more years of education; ≥ 5 for subjects with 8–15 years of education; and ≥ 3 for 0–7 years of education). Additionally, no signs of depression (geriatric depression scale, GDS score < 5) or dementia were present.

All subjects with the following clinical manifestation were excluded: (1) significant medical, neurological, or psychiatric illness; (2) a history of apparent head trauma; (3) use of non-AD-related medication known to influence cerebral function; and (4) alcohol or drug abuse. After careful screening of the data, one participant was excluded due to depression; one participant was excluded because of prominent calcification in the occipital lobe; and one participant was excluded due to excessive head motion. Table 1 presents the demographic data for the remaining 49 subjects (including 17 APOE ε4 carriers and 32 NC).

Neuropsychological assessment and APOE genotyping

All subjects underwent extensive neuropsychological batteries to assess their general mental status (MMSE) and other cognitive domains, including memory (Auditory Verbal Learning Test, AVLT; Immediate Story Recall, IST; and Delayed Story Recall, DST), processing speed/attention (Trail-Making Test, Part A, TMT-A), visuospatial function (Clock-Drawing Test, CDT), executive function (Trail-Making Test, Part B, TMT-B), and language (Boston Naming Test, BNT; Semantic Verbal Fluency, SVF).

APOE genotyping for all participants was performed as previously described (Saykin et al. 2010). In brief, APOE genotyping for all subjects was performed using DNA extracted from peripheral blood cells. The cells were collected in single EDTA plastic tubes (10 ml) and were sent via overnight delivery, at room temperature, to the University of Pennsylvania AD Biofluid Bank Laboratory.

CSF samples and quantification

Levels of $A\beta_{1-42}$, total tau (t-tau) and phosphorylated tau ($p\text{-}tau_{181}$) were measured from CSF samples, which were obtained using the standardized ADNI protocol, as previously described (Blennow et al. 2015; Shaw et al. 2016). It should be noted that not all subjects in the present study had CSF samples because lumbar puncture is an invasive procedure and is not obligatory for healthy subjects. Thus, the final samples for CSF analyses included 28 out of 32 of the APOE ε4 carriers and 14 out of the 17 NC.

Data acquisition

All participants were scanned using a 3.0-Tesla Philips MRI scanner. Structural images were acquired using a 3D MPRAGE T1-weighted sequence with the following parameters: repetition time (TR) = 2300 ms; echo time (TE) = 2.98 ms; inversion time (TI) = 900 ms; 170 sagittal slices; within plane FOV = 256 × 240 mm^2; voxel size = 1.1 × 1.1 × 1.2 mm^3; flip angle = 9°; and bandwidth = 240 Hz/pix. The T2 FLAIR scans were obtained using an echo-planar imaging sequence with the following parameters: TR = 9000 ms, TE = 90 ms, and TI = 2500 ms. The rsfMRI scans were obtained using an echo-planar imaging sequence with the following parameters: 140 time points; TR = 3000 ms; TE = 30 ms; flip angle = 80°; number of slices = 48; slice thickness = 3.3 mm; spatial resolution = 3.31 × 3.31 × 3.31 mm^3; and matrix = 64 × 64. According to the human scan protocol of the ADNI database, all subjects should have kept their eyes open with fixation (focus on a point on the mirror) during the entire rsfMRI scan.

Imaging preprocessing

Data preprocessing was performed using the Data Processing Assistant for Resting-state fMRI (DPARSF, Yan and Zang; http://rfmri.org/DPASFA), which is based on the Statistical Parametric Mapping software (SPM8) package and Resting-State fMRI Data Analysis Toolkit (REST; Song et al., http://restfmri.net). The first ten time points of the rsfMRI data were discarded due to the instability of the initial MRI signal and the subjects' adaptation to the scanning noise. The remaining 130 images were corrected for both timing differences between each slice and head motion (Friston 24 parameters). Datasets with more than 2.0 mm maximum displacement in any of the x, y, or z directions or 2.0° of any angular motion were discarded. Subsequently, based on a thorough rigid-body transformation, the T1-weighted images were co-registered to the mean rsfMRI image and spatially normalized to the Montreal Neurological Institute (MNI) stereotactic space, then resampled to 3 × 3 × 3 mm^3 cubic voxels. The functional images were spatially smoothed with a Gaussian kernel of 6 × 6 × 6 mm^3 full width at half maximum to decrease spatial noise. Finally, linear trends and temporal filtering (0.01 < f < 0.08 Hz) were performed. To remove any residual effects of motion or other non-neuronal factors, Friston 24 head motion parameters, white matter signals, and cerebrospinal fluid signals were used as nuisance

Table 1 Demographic information, neuropsychological test and neuropathological biomarker for APOE ε4 carrier and non-carriers

	ε4 carrier (n = 17)	non-carriers (n = 32)	T-value (χ^2)	P-value
Age (years)	76.09 ± 5.91	76.11 ± 5.63	1.17	0.25
Education (years)	17.53 ± 1.84	16.34 ± 2.16	− 1.92	0.06
BMI (kg/m^2)	26.48 ± 5.35	26.50 ± 4.89	0.01	0.99
Female	12	13	3.99	0.07
General mental status				
MMSE	28.94 ± 1.35	29.06 ± 1.19	0.33	0.75
Memory function				
IST	15.35 ± 2.74	14.34 ± 2.65	− 1.26	0.22
DST	14.76 ± 3.17	13.22 ± 2.53	− 1.86	0.07
AVLT 1–5 sum	42.59 ± 10.24	42.22 ± 10.38	− 0.45	0.65
Visuo-spatial processing				
CDT	4.88 ± 0.33	4.72 ± 0.52	− 1.17	0.25
Language				
SVF	21.18 ± 4.08	20.50 ± 5.41	− 0.45	0.65
Log-transformed BNT	1.46 ± 0.02	1.46 ± 0.03	0.11	0.91
Attention				
Log-transformed TMTA	1.50 ± 0.09	1.50 ± 0.11	− 1.17	0.91
Executive function				
Log-transformed TMTB	1.88 ± 0.22	1.83 ± 0.12	− 0.92	0.36
WMH (mm^3)	3.82 ± 2.98	7.24 ± 8.84	1.54	0.13
ICV	1376.02 ± 124.28	1463.68 ± 164.20	1.92	0.06
WMH/ICV (%)	0.28	0.47	1.34	0.19
Hyperintension (n)	8	11	0.75	0.54
Smoke history (n)	2	7	0.76	0.47
Diabetes (n)	0	2	1.11	0.54
CSF				
$A\beta_{1-42}$ (pg/mL)	1036.46 ± 783.54	1295.72 ± 540.92	1.26	0.22
T-tau (pg/mL)	278.77 ± 73.01	236.37 ± 82.24	− 1.70	0.10
p-tau$_{181}$ (pg/mL)	27.05 ± 8.07	22.37 ± 9.15	− 1.69	0.56

Data is presented as means ± standard deviations

It should be noted that mean level of $A\beta_{1-42}$, t-tau and p-tau$_{181}$ levels in Table only represent the subjects who had CSF sample. The final samples for CSF analyses included 28 out of 32 APOE ε4 carriers and 14 out of 17 NC

Abbreviation: MMSE Mini-Mental State Examination, *IST* Immediate Story Recall, *DST* Delayed Story Recall, *AVLT* auditory verbal learning test, *BNT* Boston naming test, *CDT* clock drawing test, *SVF* semantic verbal fluency, *TMT* Trail-Making Test, *ICV* Intracranial volume, *WMH* white matter hyperintensities

variables in the functional connectivity analysis. Given the dispute of removing the global signal in the preprocessing of rsfMRI data, we omitted to regress the global signal out. In addition, given that the two groups may differ in the occurrence of micromotion artifacts, the framewise displacement (FD) value was computed for each subject. Subjects were screened and excluded for FD values > 0.5 mm on more than 35 volumes.

Granger causality analysis

The GCA was calculated using the REST-GCA toolkit, based on Geweke's feedback model (Song et al. 2011; Geweke 1982). The GCA was used to describe the EC analysis between the PCC/aMPFC and all other brain regions. The seed areas of the PCC (2, − 51, 27) and aMPFC (− 6, 52, − 2) were performed as previously described (Greicius et al. 2003; Andrews-Hanna et al. 2010). Then, a 5-mm radius sphere centered on this coordinate was used as the seed region of the PCC/aMPFC. A lag of one TR (3000 ms) was used to assess the time-directed prediction between the rsfMRI time series of the seed regions and the rest of the brain (Hamilton et al. 2011). A signed-path coefficients algorithm in the REST-GCA toolkit was selected to obtain the GCA map.

More specifically, the averaged time series of the seed region was defined as the seed time series X, while the time series Y represented the time series of each voxel within

the whole brain (Zang et al. 2012). The linear direct effect of X on Y (information flow from X to Y) and the linear direct effect of Y on X (information flow from Y to X) were assessed within the whole brain, voxel by voxel. This concept was based on the idea that, given two time series, namely, X and Y, knowing the past of Y is useful for predicting the future of X, which means Y may have a causal influence on X. Regarding the directionality, a positive coefficient from X to Y represented that the activity in region X exerted a causal influence on the activity in region Y in the same direction. On the other hand, a negative coefficient from X to Y indicated that the activity in region X exerted an opposing directional influence on the activity of region Y (Seth et al. 2015). As a result, the GCA maps from the PCC/aMPFC to the whole brain and from the whole brain to the PCC/aMPFC for each participant were obtained.

Vascular risk factors evaluation

Vascular risk factors are likely confounded with spontaneous brain activity, particularly in an aging population. In the present study, vascular risk factors were ascertained by a self-report, which incorporated current or past diagnoses, treatment of diabetes or hypertension, and smoking status.

In addition, the white matter hyperintensities (WMH) burden of every subject was taken into consideration in the current research. Our previous WMH segmentation methods were used, and we briefly described the process here (Luo et al. 2017). For each subject, a WMH lesion map was automatically created based on the 3D MPRAGE T1-weighted and T2 FLAIR images using the Lesion Segmentation Toolbox. The masks were then manually corrected by two experienced neuroradiologists (MMZ, HPY). Then, we coregistered the 3D MPRAGE T1, T2 FLAIR and the corrected masks to the standard atlas (UNC adult brain atlas template, http://www.nitrc.org). Finally, the WMH volume of each participant was calculated; meanwhile, we also estimated the total intracranial volume (ICV).

Evaluation of the impact of physiological noise

Although the frequency of the physiological data fell outside of the range 0.01–0.08 Hz, a previous study showed that in areas with high blood volumes, such as the blood vessels and gray matter, the effect of physiological noise may cause changes in the BOLD signal (Birn et al. 2014). To examine the impact of physiological noise (e.g., cardiac and respiratory fluctuations), we also calculated the correlation between the signal values from the white matter and ventricles (presumably dominated by physiologic noise (Chai et al. 2012; Chang and Glover 2009)), and the voxel-size signal value in all subjects, based on four-time GCA mapping (from the PCC to the whole brain; from the whole brain to the PCC; from the aMPFC to the whole brain; and from the whole brain to the aMPFC). Moreover, Pearson correlation analyses were performed between regions with significant GCA differences and the presumable signal value of physiological noise.

Statistical analysis

Quantitative variables are expressed as the mean and standard deviation. The categorical variables are given as absolute and relative frequencies. All statistical analyses were performed using IBM SPSS19 statistical software for Windows. The TMT-A/B and BNT performances were log-transformed due to positively skewed distribution. Group differences in terms of age, education level, and neuropathological and neuropsychological scores were examined by two-sample t-tests. Meanwhile, gender and self-reported vascular risk factors were analyzed by using a Chi square test.

The statistical analyses of GCA were performed using the REST software. To be specific, for estimating the time-directed prediction between the time series of a seed region and the rest of the whole brain, a time lag of one TR (3000 ms) was used. First, a group mask was generated to include all voxels presented across all subjects in our study (in MNI 152 standard space). All subjects' masks were multiplied to produce the group mask, and the group analyses of EC were then constrained within the group mask at the voxel level. Then, under the respective causal effects mask, GC maps of two groups from the seed regions to the whole brain (**from X to Y**) were then subjected to a two-sample t-test with age, gender, and education level as covariates, corrected for multiple comparisons by using 3dClustSim in the AFNI command line (for the PCC, voxel-height threshold $p < 0.01$, cluster = 35, corrected by $p < 0.01$; for the aMPFC, voxel-height threshold $p < 0.01$, cluster = 18, corrected by $p < 0.01$); meanwhile, the GC maps of the two groups from the whole brain to the seed regions (**from Y to X**) were analyzed using two-sample t-tests with age, gender and education level as covariates, corrected for another AlphaSim correction (for the PCC, voxel-height threshold $p < 0.01$, cluster = 13, corrected by $p < 0.01$; for the aMPFC, voxel-height threshold $p < 0.01$, cluster = 11, corrected by $p < 0.01$) (Cox 1996).

Moreover, we investigated the associations between the imaging measures and the behavioral/neuropathological data of all subjects and of the two groups separately. It should be noted that the correlations were performed only within the regions exhibiting significant EC differences between groups. Given the effects of multiple comparisons, the statistical significance level for the correlation analyses was strictly chosen as $p < 0.005$.

Results

Demographics, neuropsychological and neuropathological measures

No statistically significant differences were found in terms of gender composition, age, or education level between the APOE ε4 carriers and the non-carriers ($p > 0.05$). Additionally, concerning the micromotion data, no significant differences in the mean FD values were observed. Although the APOE ε4 allele carriers had an increased trend of tau protein (t-tau_{181} and p-tau), as well as a decreased trend of $A\beta_{1-42}$, relative to non-carriers, there were no significant differences between the groups. More detailed information can be found in Table 1.

Vascular risk factors

No statistically significant differences were found in terms of the vascular profiles between the two groups, including the prevalence of hypertension, diabetes mellitus and a history of smoking ($p > 0.05$). Moreover, no significant differences in the WMH burden (as a percentage of ICV) were found. This result suggested that vascular-related effects could not make a marked contribution to the following findings of GCA. More detailed information can be found in Table 1.

Effective connectivity

Compared with the non-carriers, the APOE ε4 carriers displayed decreased effective connectivity from the PCC to the whole brain in the left middle temporal gyrus (MTG), the right anterior cingulate cortex (ACC), and the right precuneus (PCu). However, no significant difference was found from the whole brain to the PCC between groups.

No significant difference was found from the aMPFC to the whole brain between groups. Compared with the non-carriers, the APOE ε4 carriers displayed increased EC from the entire brain to the aMPFC in the left inferior parietal lobe (IPL) and the right postcentral gyrus (PCG). More detailed information can be found in Figs. 1, 2 and Table 2.

Influence of physiologic noise on effective connectivity

Consistent with the findings of previous studies, visual inspection demonstrated that potential physiological noise was negatively associated with posterior brain regions (the parietal and occipital lobes) in the GCA map from the PCC to the whole brain. Meanwhile, potential physiological noise was positively associated with anterior regions (frontal lobe) in the GCA map from the whole brain to the aMPFC (Supplement Fig. 1). Subsequently, Pearson correction analyses were performed between the regions with significant GCA differences in the current study and potential physiological noise (signal values from the white matter and ventricles). No significant correlations were found ($p > 0.05$, Supplement Fig. 2). These results suggested that the GCA results in the current study were not mainly effects of physiological noise.

Correlations of effective connectivity and behavioral/neuropathological data

Moreover, we investigated the associations of the imaging measures and behavioral/neuropathological data in all subjects and the two groups separately, with gender and education level as covariates (close to the significant differences). The brain regions with significantly different EC between the groups were chosen as ROIs, and the average values of the ROI from the GCA map of each participant were calculated.

In all subjects, no correlative relationships between EC and cognition/CSF biomarkers were observed ($p > 0.005$). In the NC subjects, our correlation analyses revealed that the EC of the IPL (causal influence from the IPL to the aMPFC) was moderately related to episodic memory performance, including the IST ($r = 0.63$, $p < 0.001$) and the DST ($r = 0.60$, $p < 0.001$); meanwhile, the EC of the PCG (causal influence from the PCG to the aMPFC) was also significantly related to the IST ($r = 0.65$, $p < 0.001$) and DST ($r = 0.54$, $p < 0.005$). For APOE ε4 carriers, the EC of the right ACC (causal influence from the PCC to the ACC) was strongly related to the level of t-tau ($r = -0.80$, $p < 0.001$) and p-tau ($r = -0.74$, $p < 0.005$). More detailed information can be found in Fig. 3.

Discussion

To the best of our knowledge, this is the first study to demonstrate differences in whole-brain EC of healthy APOE ε4 allele carriers and non-carriers. Reduced EC from the PCC to the whole brain was revealed in the ACC, the MTG, and the PCu in ε4 carriers, compared to the NC; meanwhile, the ε4 carriers exhibited increased EC from the entire brain to the aMPFC in the IPL and the PCG. Significant correlations were found between episodic memory and visuospatial function and EC. Moreover, the level of tau protein was significantly related to the EC from the PCC to the ACC. Conclusively, our study presented a hypothesized dynamic model of the intrinsic brain network in APOE ε4 carriers; a putative downward system of negative influence could be traced from the PCC to both the posterior and anterior DMN subsystems; meanwhile, the anterior DMN subsystem received positive compensatory influence from the parietal cortex. Finally, we further

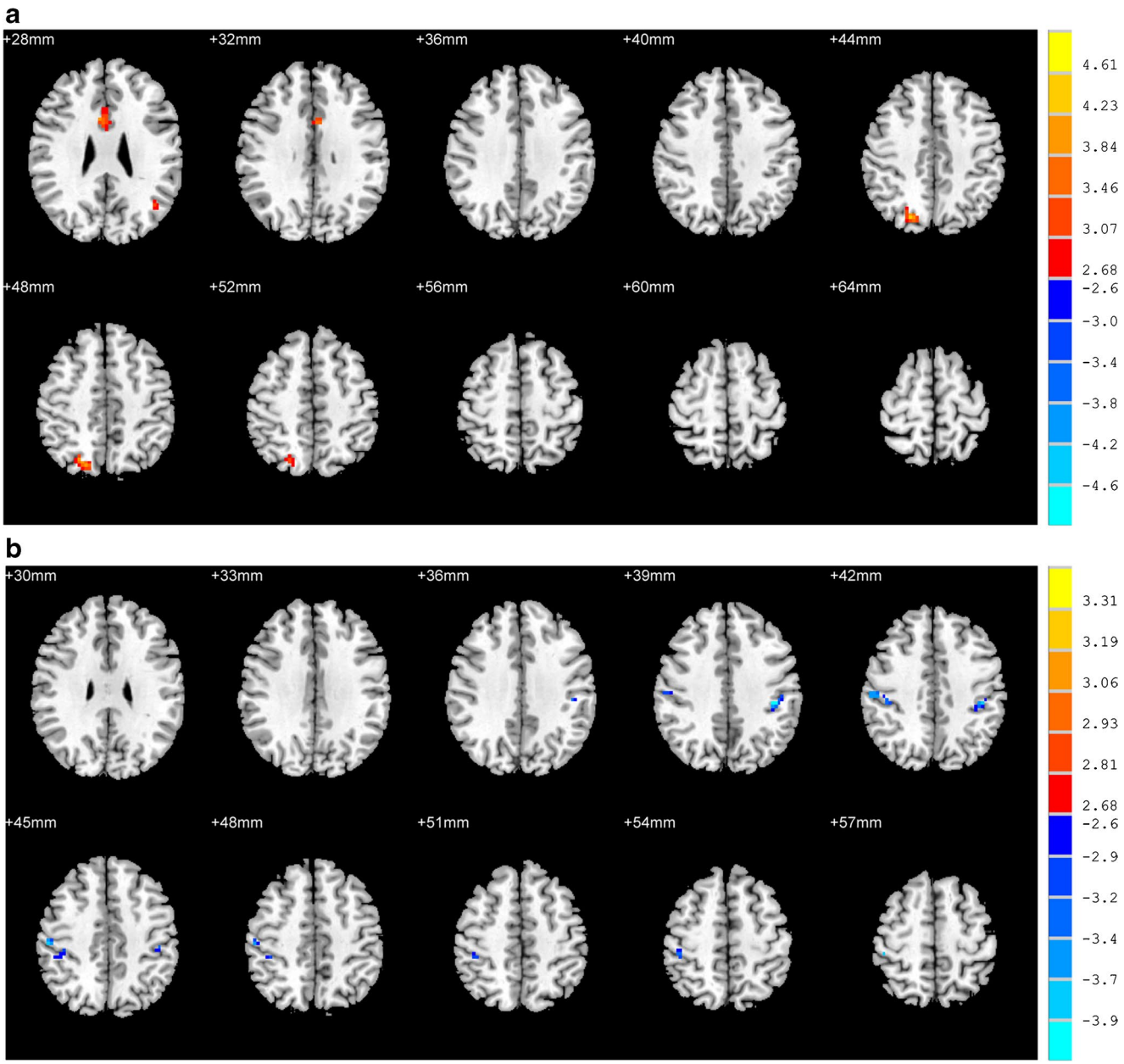

Fig. 1 **a** Brain regions showing group differences in the causal effect from the posterior cingulate cortex to the whole brain (Non-carriers VS. APOE ε4 carriers, $p < 0.01$, corrected). **b** Brain regions showing group differences in the causal effect from the whole brain to the anterior medial prefrontal cortex (Non-carriers VS. APOE ε4 carriers, $p < 0.01$, corrected)

speculated that APOE ε4 allele-related increases in NFTs might act as an initial factor during this dynamic process.

As a core hub, the PCC has reciprocal functional connections with each component of the DMN (Buckner et al. 2008; Fransson and Marrelec 2008; Raichle 2015). Previous studies of GCA conducted in healthy volunteers also demonstrated that the PCC works as the primary emitter and terminal receiver of causal influences within the whole brain (Yan et al. 2013; Miao et al. 2011). The most prominent result of our findings was that there was a reduced causal influence from the PCC to the ACC in ε4 carriers. Recently, decreased structural and functional integration of the DMN in healthy ε4 allele carriers has frequently been reported (Luo et al. 2016a, b; Goryawala et al. 2015; Brown et al. 2011). However, there were no previous studies that approached the question of what the sequential order of the process of DMN disconnection is. For the first time, the present study suggested that, at the earliest stages of AD, healthy APOE ε4

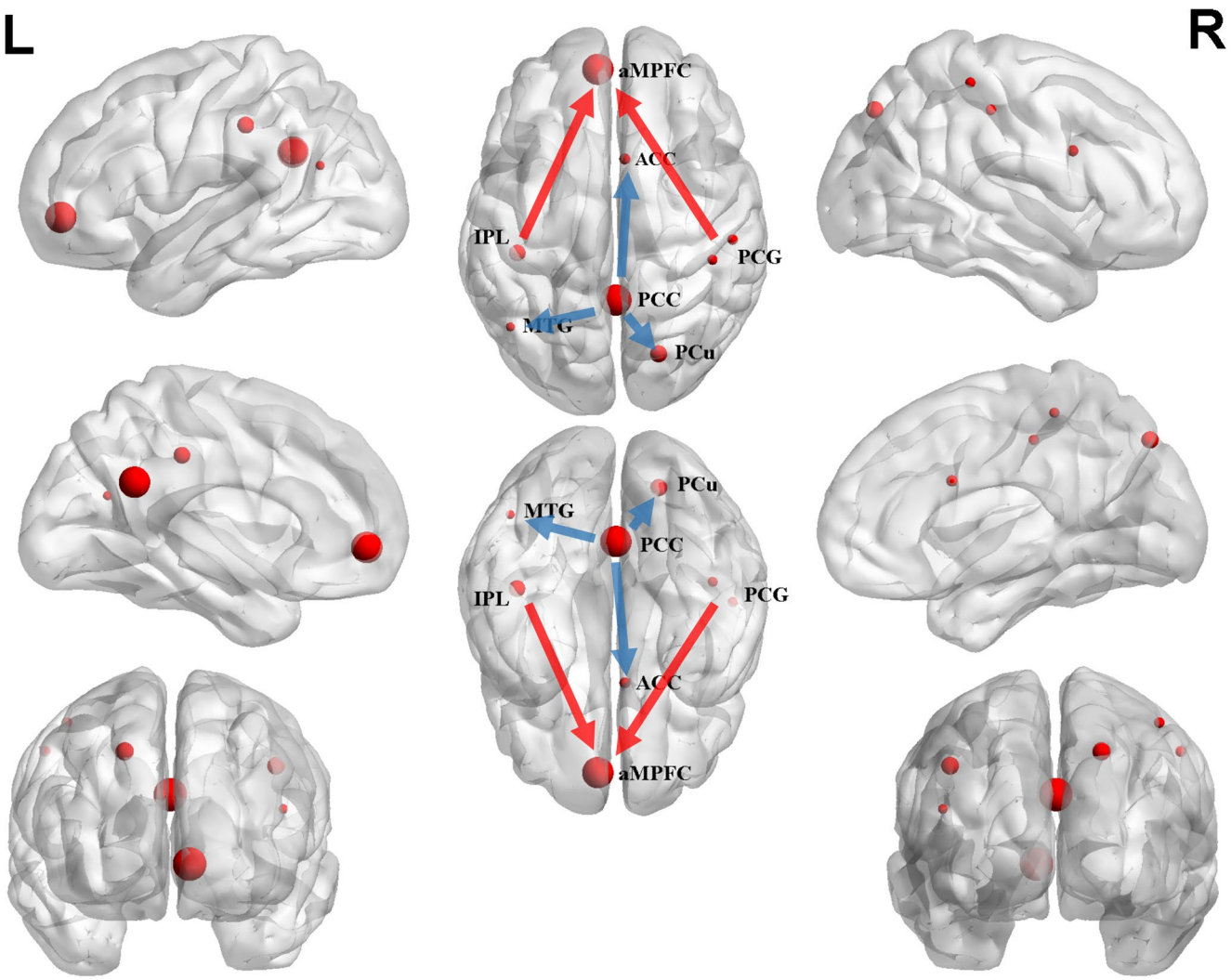

Fig. 2 B: Sketch map of the between-group differences in causal connectivity: non-carriers VS. APOE ε4 carriers. The arrow of the significant causal paths represents the direction of the information flow, and the thickness and spherical radius represent the strength of the causal connectivity. Seed points in the PCC (2, −51, 27) and the aMPFC (−6, 52, −2), adapted from previously published articles (Greicius et al. 2003; Andrews-Hanna et al. 2010). Abbreviation: PCC, posterior cingulate cortex; PCu, precuneus; MTG, middle temporal gyrus; ACC, anterior cingulate cortex; aMPFC, anterior medial prefrontal cortex; IPL, inferior parietal lobe; PCG, postcentral gyrus. For APOE ε4 carriers, the blue arrow represents reduced effective connectivity, while the red arrow indicates increased effective connectivity

Table 2 Significant group differences in granger causality analysis between non-carriers and ε4 carriers

Region (Non-carriers vs. ε4 carriers)	MNI coordinate			Cluster voxels	Peak intensity
	X	Y	Z		
Outflow from the PCC to whole brain					
Left middle temporal gyrus	−45	−63	21	50	3.85
Right anterior cingulate cortex	6	12	27	36	3.96
Right precuneus	21	−75	45	42	4.27
Outflow from the MPFC to whole brain	No significant differences				
The whole brain inflow to the MPFC					
Left Inferior parietal lobe	−42	−30	39	21	−4.25
Right postcentral gyrus	54	−24	45	16	−3.93
Right postcentral gyrus	45	−33	57	21	−3.91
The whole brain inflow to the PCC	No significant differences				

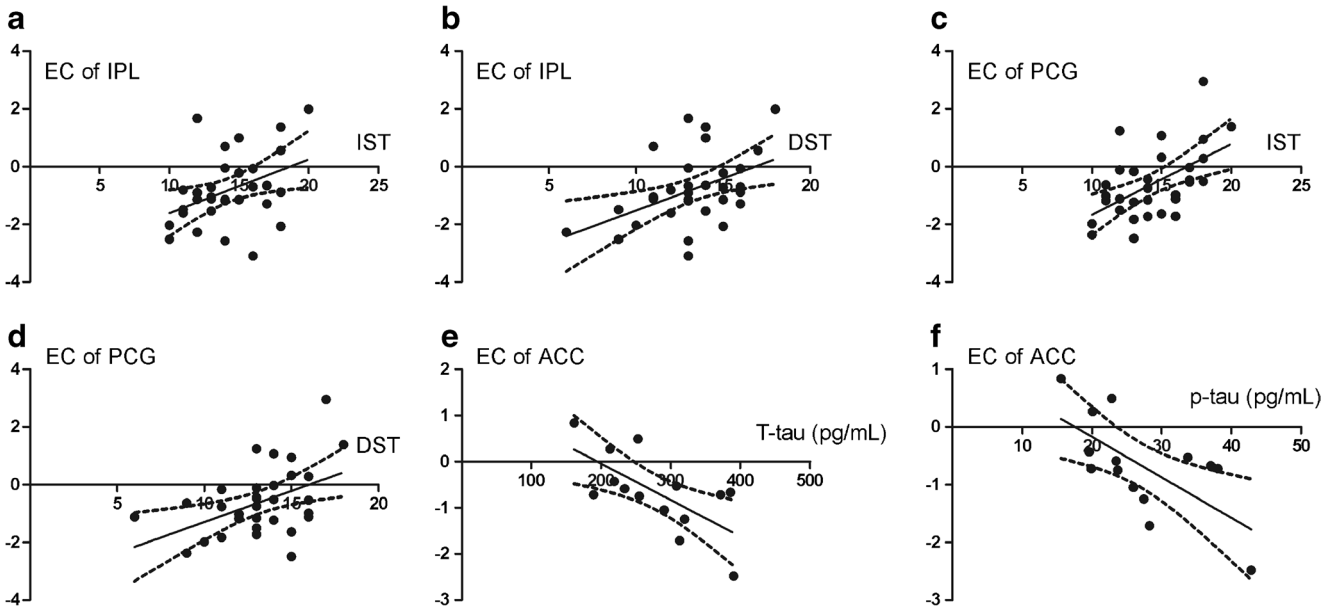

Fig. 3 Scatter plot diagram of the correlation between effective connectivity and neuropathological data/AD-related pathology. **a/b**: In NC subjects, our correlation analyses revealed that the EC of the IPL (causal influence from the IPL to the aMPFC) was moderately related to episodic memory performance, including the IST ($r=0.63$, $p<0.001$) and the DST ($r=0.60$, $p<0.001$). **c/d**: meanwhile, the EC of the PCG (causal influence from the PCG to the aMPFC) was also significantly related to the IST ($r=0.65$, $p<0.001$) and the DST ($r=0.54$, $p<0.005$); **e/f**: In the APOE ε4 carriers, the EC of the right ACC (causal influence from the PCC to the ACC) was strongly related to the levels of t-tau ($r=-0.80$, $p<0.001$) and p-tau ($r=-0.74$, $p<0.005$). Abbreviation: ACC, anterior cingulate cortex; IPL, inferior parietal lobe; PCG, postcentral gyrus

carriers exhibited a negative causal influence from the posterior to the anterior DMN subsystem (Sperling et al. 2011). Supportive neuropathologic evidence comes from the work of Braak et al., who documented that selective distribution of AD-related pathologies begin to aggregate in regions located in the posterior DMN then spread to the front of the brain (Braak et al. 2006).

Both the MTG and the PCu are part of the posterior DMN, which is closely related to the extraction of episodic memory (Fransson and Marrelec 2008). Functionally, a neuroimaging study showed that the PCC has extensive projections to the regions of the MTG and the PCu in healthy subjects (Jiao et al. 2011). However, our results indicated that ε4 allele carriers had reduced causal influence from the PCC to the MTG/PCu. These results suggest that, apart from the disconnection between the anterior and posterior DMN subsystems, ε4 allele carriers still had a regional disconnection within the posterior subsystem of the DMN. In AD preclinical subjects, our findings coincided and extended previous GCA studies documenting that amnestic MCI patients had decreased causal connectivity from the PCC to regions of the MTL (Yan et al. 2013; Yang et al. 2017). In addition, it is interesting to note that there were no differences in the EC from the whole brain to the PCC. In contrast, previous GCA studies conducted with AD or MCI patients have reported reduced EC from the hippocampus to the PCC (Wu et al. 2011; Liang et al. 2014). We inferred that the negative result suggested that the PCC in ε4 carriers still reserves normal function in receiving incoming information from the whole brain.

Our results showed that APOE ε4 carriers demonstrated a positive causal influence from the left IPL and the right PCG to the aMPFC, the second hub of the DMN (Buckner et al. 2009). Previous studies of EC have shown that there is a potential moderating role for the IPL in the anterior DMN subsystem. Specifically, Zhou et al. utilized GCA and found a causal influence from the left IPL to the MPFC in healthy subjects (Zhou et al. 2011); another study using dynamic causal modeling also reported that information flows from the bilateral IPL to the MPFC region (Di and Biswal 2014). On the other hand, the major function of the PCC is somatosensory processing, such as the somatic sensation of external stimuli (Nelson and Chen 2008). However, it should be noted that the parietal cortex has extensive connections with the frontal lobe region (i.e., the parieto-frontal circuit), which could send rich sensory information not only for movement control but also for other cognitive abilities (Buckner et al. 2009). Conclusively, it is evident that the driving effects from the IPL/PCG to the aMPFC were enhanced, which may compensate for the cognitive abilities that should have been disrupted in APOE ε4 carriers.

Subsequent correlation analyses in the NC subjects showed that the EC from the IPL/PCG to the aMPFC was moderately related to the performance of episodic memory, even after being corrected for gender and education level. These results were in line with the recent notion that the parietal cortex supports an additional role in episodic memory retrieval (Sestieri et al. 2017). However, these correlations were not found in APOE ε4 carriers, and there was no difference in the memory function between the two groups. These results further supported our hypothesis that the enhanced causal influence of the anterior DMN subsystem may reflect recruitment of the parietal cortex as a compensatory mechanism. It has been shown that elderly subjects traditionally recruit more parietal regions to counteract the neurobiological changes due to aging or disease (Marion et al. 2003).

Consistent with most studies regarding the APOE genotype, we found no differences in the behavioral data between the APOE ε4 carriers and non-carriers (Luo et al. 2017; Alexander et al. 2007; Westlye et al. 2011). This finding may indicate that neuropsychological batteries may not be sensitive enough to reliably capture the most APOE ε4-specific gene-expression profiles (compared to assessing EC). Meanwhile, given that the mean education level of the APOE ε4 carriers (17.5 years) in the current study was higher than that in other studies, the negative result of behavioral data could be interpreted by the theory of cognitive reserve (CR). Specifically, this suggests that an individual with high cognitive reserve (e.g., higher education) would cope better with the same amount of pathology than an individual with low CR and a delay in the onset of symptoms (Stern 2012; Meng and Carl 2012).

CSF biomarkers, including Aβ1-42, t-tau, and p-tau181, are also useful biomarker candidates, as they are intimately related to amyloid plaques, neuronal death and accumulation of tangles (Galasko and Shaw 2017). As an exploratory analysis, we further examined the relationship between the mean EC in regions with significant differences between the groups and CSF biomarkers. Our results revealed that the EC of the right ACC (causal influence from PCC to ACC) was strongly related to the levels of t-tau ($r = -0.80$) and p-tau ($r = -0.74$) in the APOE ε4 carriers. Accordingly, we speculated that deficits in EC might be a consequence of the early events of APOE ε4 allele-mediated reductions in the efficiency of unphosphorylated binding tau (Jiang et al. 2008). It is known that AD-related pathological processes span decades; the distribution pattern of the lesions develops according to a predictable sequence during this neuropathological process (Braak et al. 2006). Pathologically, as the core hub of the DMN, the PCC is preferentially affected with AD-related neurofibrillary tangles (NFTs) relative to other regions (Buckner et al. 2009). As a result, early accumulations of NFTs may impair the neuropil of the PCC; we then observed decreased EC from the posterior to anterior DMN subsystems (Whitwell et al. 2008). However, it should be noted that without direct histological data, such interpretations should be made with caution.

There existed several limitations to this study. First, this cross-sectional study lacked clinical follow-up information to make any possible inferences between the current findings and AD, and thus, longitudinal studies are needed to determine whether decreased or increased causal influences are associated with a higher risk of developing AD-related pathological changes. Second, though all the rsfMRI data were temporally bandpass filtered (0.01–0.08 Hz), and the results of the present study were not mainly effects of physiological noise, we still cannot completely remove the effects of physiological noise on our findings (Birn et al. 2006). Accordingly, future studies should record the heart rate, and the respiratory rate and depth simultaneously during rsfMRI scanning to control for physiological noise. Third, previous studies confirmed that carrying APOE E4 allele causes a dose-dependent increase in the risk of developing AD (Corder et al. 1993). However, due to an insufficient number of cognitively intact E4 homozygotes in the ADNI database, the E4 group was not divided into E4 homozygotes and heterozygotes in the current study. It would be meaningful to explore the dose-dependent effects of the E4 allele on EC in future studies. Finally, although GCA has the potential to shed light on the characterization of functional circuits, it should be noted that applications of GCA based on rsfMRI data are not yet part of a standard conceptual toolkit; there are still some controversial problems, especially for the low sampling rate (equal to MRI repetition time) relative to neuronal responses, and the potential confounding hemodynamic delays (Friston et al. 2013; Seth et al. 2015). Future studies should pay more attention to ensure the data and analysis process respect the necessary assumptions and make interpretations with caution.

Conclusion

To the best of our knowledge, this is the first study that used GCA to analyze the APOE ε4-related effects on whole-brain connectivity in healthy elderly populations. First, we observed that the presence of the APOE ε4 allele was linked to reduced EC from the PCC to the anterior and posterior DMN subsystems; additionally, the APOE ε4 allele was also associated with increased EC from the parietal cortex to the anterior DMN subsystem. Second, the correlation analyses indicated that the decreased EC in the APOE ε4 carriers might result from neuronal death caused by toxicity due to neurofibrillary changes. Finally, we demonstrated that GCA is sensitive to APOE genotype differences several years before the occurrence of dementia symptoms.

Acknowledgements Data collection and sharing for this project was funded by the Alzheimer's Disease Neuroimaging Initiative (ADNI) (National Institutes of Health Grant U01 AG024904) and DOD ADNI (Department of Defense award number W81XWH-12-2-0012). ADNI is funded by the National Institute on Aging, the National Institute of Biomedical Imaging and Bioengineering, and through generous contributions from the following: AbbVie, Alzheimer's Association; Alzheimer's Drug Discovery Foundation; Araclon Biotech; Bio Clinica, Inc.;Biogen; Bristol-Myers Squibb Company; Cere Spir, Inc.; Eisai Inc.; Elan Pharmaceuticals, Inc.; Eli Lilly and Company; Euro Immun; F. Hoffmann-La Roche Ltd and its affiliated company Genentech, Inc.; Fujirebio; GE Healthcare; IXICO Ltd.; Janssen Alzheimer Immunotherapy Research & Development, LLC.; Johnson & Johnson Pharmaceutical Research & Development LLC.; Lumosity; Lundbeck; Merck & Co., Inc.; MesoScale Diagnostics, LLC.; NeuroRx Research; Neurotrack Technologies; Novartis Pharmaceuticals Corporation; Pfizer Inc.; Piramal Imaging; Servier; Takeda Pharmaceutical Company; and Transition Therapeutics. The Canadian Institutes of Health Research is providing funds to support ADNI clinical sites in Canada. Private sector contributions are facilitated by the Foundation for the National Institutes of Health (http://www.fnih.org). The grantee organization is the Northern California Institute for Research and Education, and the study is coordinated by the Alzheimer's Disease Cooperative Study at the University of California, San Diego. ADNI data are disseminated by the Laboratory for Neuroimaging at the University of Southern California.

Author Contributions Xiao Luo, Kaicheng Li and Yunlu Jia were contributed equally to this work. The data used in the preparation of this article were obtained from the Alzheimer's Disease Neuroimaging Initiative (ADNI) database (http://www.adni.loni.usc.edu). As such, the investigators within the ADNI contributed to the design and implementation of ADNI and provided data but did not participate in the analysis or writing of this report. A complete listing of the ADNI investigators can be found in the supplement.

Funding This study was funded by National Key Research and Development Program of China (NO.2016YFC1306600), Fundamental Research Funds for the Central Universities (NO. 2017XZZX001-01), Zhejiang Provincial Natural Science Foundation of China (Grant NO. LZ14H180001), Projects of Medical and Health Technology Development Program in Zhejiang Province (2015KYB174), Young Talents Research Fund, Chinese Medicine Science and Technology Project of Zhejiang Province (No. 2018ZQ035).

Compliance with ethical standards

Conflict of interest The authors declare no conflict of interest.

Ethical approval All procedures performed in studies involving human participants were in accordance with the ethical standards of the institutional and/or national research committee and with the 1964 Helsinki declaration and its later amendments or comparable ethical standards.

Informed consent Written informed consent was obtained from all participants and/or authorized representatives and the study partners before any protocol-specific procedures were carried out in the ADNI study.

References

Alexander, D. M., Williams, L. M., Gatt, J. M., Dobson-Stone, C., Kuan, S. A., Todd, E. G., et al. (2007). The contribution of apolipoprotein E alleles on cognitive performance and dynamic neural activity over six decades. *Biological Psychology, 75*(3), 229–238.

Andrews-Hanna, J. R. (2012). The brain's default network and its adaptive role in internal mentation. *The Neuroscientist, 18*(3), 251–270.

Andrews-Hanna, J. R., Reidler, J. S., Sepulcre, J., Poulin, R., & Buckner, R. L. (2010). Functional-anatomic fractionation of the brain's default network. *Neuron, 65*(4), 550–562.

Birn, R. M., Cornejo, M. D., Molloy, E. K., Patriat, R., Meier, T. B., Kirk, G. R., et al. (2014). The influence of physiological noise correction on test–retest reliability of resting-state functional connectivity. *Brain Connectivity, 4*(7), 511–522.

Birn, R. M., Diamond, J. B., Smith, M. A., & Bandettini, P. A. (2006). Separating respiratory-variation-related fluctuations from neuronal-activity-related fluctuations in fMRI. *Neuroimage, 31*(4), 1536–1548.

Blennow, K., Teunissen, C. E., Ostlund, R. E., Militello, M., Zetterberg, H., Hubeek, I., et al. (2015). Multicentre performance evaluation of a novel, fully automated electrochemiluminescence immunoassay for the quantitation of Aβ(1–42) in human cerebrospinal fluid. *Alzheimers & Dementia the Journal of the Alzheimers Association, 11*(7), P295-P296.

Braak, H., Alafuzoff, I., Arzberger, T., Kretzschmar, H., & Del Tredici, K. (2006). Staging of Alzheimer disease-associated neurofibrillary pathology using paraffin sections and immunocytochemistry. *Acta Neuropathologica, 112*(4), 389–404.

Brown, J. A., Terashima, K. H., Burggren, A. C., Ercoli, L. M., Miller, K. J., Small, G. W., et al. (2011). Brain network local interconnectivity loss in aging APOE-4 allele carriers. *Proceedings of the National Academy of Sciences of the United States of America, 108*(51), 20760–20765.

Buckner, R. L., Andrews-Hanna, J. R., & Schacter, D. L. (2008). The brain's default network: anatomy, function, and relevance to disease. *Annals of the New York Academy of Sciences, 1124*(1), 1–38.

Buckner, R. L., Sepulcre, J., Talukdar, T., Krienen, F. M., Liu, H., Hedden, T., et al. (2009). Cortical hubs revealed by intrinsic functional connectivity: mapping, assessment of stability, and relation to Alzheimer's disease. *Journal of Neuroscience, 29*(6), 1860–1873.

Chai, X. J., Castañón, A. N., Öngür, D., & Whitfield-Gabrieli, S. (2012). Anticorrelations in resting state networks without global signal regression. *Neuroimage, 59*(2), 1420–1428.

Chang, C., & Glover, G. H. (2009). Effects of model-based physiological noise correction on default mode network anti-correlations and correlations. *Neuroimage, 47*(4), 1448–1459.

Corder, E., Saunders, A., Strittmatter, W., Schmechel, D., Gaskell, P., Small, G. A., et al. (1993). Gene dose of apolipoprotein E type 4 allele and the risk of Alzheimer's disease in late onset families. *Science, 261*(5123), 921–923.

Cox, R. W. (1996). AFNI: software for analysis and visualization of functional magnetic resonance neuroimages. *Computers and Biomedical Research, 29*(3), 162–173.

Di, X., & Biswal, B. B. (2014). Identifying the default mode network structure using dynamic causal modeling on resting-state functional magnetic resonance imaging. *Neuroimage, 86*(2), 53–59.

Farfel, J. M., Yu, L., De Jager, P. L., Schneider, J. A., & Bennett, D. A. (2016). Association of APOE with tau-tangle pathology with and without β-amyloid. *Neurobiology of Aging, 37*, 19.

Fransson, P., & Marrelec, G. (2008). The precuneus/posterior cingulate cortex plays a pivotal role in the default mode network: Evidence from a partial correlation network analysis. *Neuroimage, 42*(3), 1178–1184.

Friston, K., Moran, R., & Seth, A. K. (2013). Analysing connectivity with Granger causality and dynamic causal modelling. *Current Opinion in Neurobiology, 23*(2), 172–178.

Friston, K. J. (2011). Functional and effective connectivity: a review. *Brain Connectivity, 1*(1), 13–36.

Galasko, D. R., & Shaw, L. M. (2017). Alzheimer disease: CSF biomarkers for Alzheimer disease - approaching consensus. *Nature Reviews Neurology, 13*(3), 131.

Geweke, J. (1982). Measurement of linear dependence and feedback between multiple time series. *Journal of the American Statistical Association, 77*(378), 304–313.

Goryawala, M., Duara, R., Loewenstein, D. A., Zhou, Q., Barker, W., Adjouadi, M., et al. (2015). Apolipoprotein-E4 (ApoE4) carriers show altered small-world properties in the default mode network of the brain. *Biomedical Physics & Engineering Express, 1*(1), 015001.

Granger, C. W. (1969). Investigating causal relations by econometric models and cross-spectral methods. *Econometrica: Journal of the Econometric Society*, 424–438.

Greicius, M. D., Krasnow, B., Reiss, A. L., & Menon, V. (2003). Functional connectivity in the resting brain: a network analysis of the default mode hypothesis. *Proceedings of the National Academy of Sciences, 100*(1), 253–258.

Hamilton, J. P., Chen, G., Thomason, M. E., Schwartz, M. E., & Gotlib, I. H. (2011). Investigating neural primacy in Major Depressive Disorder: multivariate Granger causality analysis of resting-state fMRI time-series data. *Molecular Psychiatry, 16*(7), 763–772.

Jiang, Q., Lee, C. D., Mandrekar, S., Wilkinson, B., Cramer, P., Zelcer, N., et al. (2008). ApoE promotes the proteolytic degradation of Ab. *Neuron, 58*(5), 681–693.

Jiao, Q., Lu, G., Zhang, Z., Yuan, Z., Wang, Z., Guo, Y., et al. (2011). Granger causal influence predicts BOLD activity levels in the default mode network. *Human Brain Mapping, 32*(1), 154–161.

Liang, P., Li, Z., Deshpande, G., Wang, Z., Hu, X., & Li, K. (2014). Altered causal connectivity of resting state brain networks in amnesic MCI. *PloS One, 9*(3), e88476.

Liu, C. C., Kanekiyo, T., Xu, H., & Bu, G. (2013). Apolipoprotein E and Alzheimer disease: risk, mechanisms and therapy. *Nature Reviews Neurology, 9*(2), 106.

Luo, X., Jiaerken, Y., Huang, P., Xu, X. J., Qiu, T., Jia, Y., et al. (2017). Alteration of regional homogeneity and white matter hyperintensities in amnestic mild cognitive impairment subtypes are related to cognition and CSF biomarkers. *Brain Imaging and Behavior*, 1–13.

Luo, X., Jiaerken, Y., Yu, X., Huang, P., Qiu, T., Jia, Y., et al. (2017). Associations between APOE genotype and cerebral small-vessel disease: a longitudinal study. *Oncotarget*.

Luo, X., Qiu, T., Jia, Y., Huang, P., Xu, X., Yu, X., et al. (2016a). Intrinsic functional connectivity alterations in cognitively intact elderly APOEe4 carriers measured by eigenvector centrality mapping are related to cognition and CSF biomarkers: a preliminary study. *Brain Imaging and Behavior*, 1–12.

Luo, X., Qiu, T., Xu, X., Huang, P., Gu, Q., Shen, Z., et al. (2016b). Decreased inter-hemispheric functional connectivity in cognitively intact elderly APOE ε4 carriers: a preliminary study. *Journal of Alzheimer's Disease, 50*(4), 1137–1148.

Machulda, M. M., Jones, D. T., Vemuri, P., Mcdade, E., Avula, R., Przybelski, S., et al. (2011). Effect of APOE e4 status on intrinsic network connectivity in cognitively normal elderly subjects. *Archives of Neurology, 68*(9), 1131.

Marion, S. D., Kilian, S. C., Naramor, T. L., & Brown, W. S. (2003). Normal development of bimanual coordination: visuomotor and interhemispheric contributions. *Developmental Neuropsychology, 23*(3), 399–421.

Mckenna, F., Koo, B. B., & Killiany, R. (2015). Comparison of ApoE-related brain connectivity differences in early MCI and normal aging populations: an fMRI study. *Brain Imaging & Behavior*, 1–14.

Meng, X., & Carl, D. A. (2012). Education and dementia in the context of the cognitive reserve hypothesis: a systematic review with meta-analyses and qualitative analyses. *PloS One, 7*(6), e38268.

Miao, X., Wu, X., Li, R., Chen, K., & Yao, L. (2011). Altered connectivity pattern of hubs in default-mode network with Alzheimer's disease: an Granger causality modeling approach. *PloS One, 6*(10), e25546.

Montine, T. J., Monsell, S. E., Beach, T. G., Bigio, E. H., Bu, Y., Cairns, N. J., et al. (2016). Multisite assessment of NIA-AA guidelines for the neuropathologic evaluation of Alzheimer's disease. *Alzheimers & Dementia the Journal of the Alzheimers Association, 12*(2), 164.

Nelson, A. J., & Chen, R. (2008). Digit somatotopy within cortical areas of the postcentral gyrus in humans. *Cerebral Cortex, 18*(10), 2341–2351.

Padayachee, E. R., Zetterberg, H., Portelius, E., Borén, J., Molinuevo, J. L., Andreasen, N., et al. (2016). Cerebrospinal fluid-induced retardation of amyloid baggregation correlates with Alzheimer's disease and the APOE e4 allele. *Brain Research, 1651*, 11–16.

Persson, J., Lind, J., Larsson, A., Ingvar, M., Sleegers, K., Van, B. C., et al. (2008). Altered deactivation in individuals with genetic risk for Alzheimer's disease. *Neuropsychologia, 46*(6), 1679–1687.

Raichle, M. E. (2015). The brain's default mode network. *Annual Review of Neuroscience, 38*, 433–447.

Saykin, A. J., Shen, L., Foroud, T. M., Potkin, S. G., Swaminathan, S., Kim, S., et al. (2010). Alzheimer's Disease Neuroimaging Initiative biomarkers as quantitative phenotypes: genetics core aims, progress, and plans. *Alzheimer's & Dementia, 6*(3), 265–273.

Sestieri, C., Shulman, G. L., & Corbetta, M. (2017). The contribution of the human posterior parietal cortex to episodic memory. *Nature Reviews Neuroscience, 18*(3), 183–192.

Seth, A. K., Barrett, A. B., & Barnett, L. (2015). Granger causality analysis in neuroscience and neuroimaging. *Journal of Neuroscience, 35*(8), 3293–3297.

Shaw, L. M., Fields, L., Korecka, M., Waligórska, T., Trojanowski, J. Q., Allegranza, D., et al. (2016). Method comparison of AB(1–42) measured in human cerebrospinal fluid samples by liquid chromatography-tandem mass spectrometry, the Inno-Bia ALZBIO3 assay, and the Elecsys® B-amyloid(1–42) assay. *Alzheimers & Dementia the Journal of the Alzheimers Association, 12*(7), P668-P668.

Song, X.-W., Dong, Z.-Y., Long, X.-Y., Li, S.-F., Zuo, X.-N., Zhu, C.-Z., et al. (2011). REST: a toolkit for resting-state functional magnetic resonance imaging data processing. *PloS One, 6*(9), e25031.

Sperling, R. A., Aisen, P. S., Beckett, L. A., Bennett, D. A., Craft, S., Fagan, A. M., et al. (2011). Toward defining the preclinical stages of Alzheimer's disease: recommendations from the National Institute on Aging-Alzheimer's Association workgroups on diagnostic guidelines for Alzheimer's disease. *Alzheimers & Dementia, 7*(3), 280.

Stern, Y. (2012). Cognitive reserve in ageing and Alzheimer's disease. *Lancet Neurology, 11*(11), 1006.

Suri, S., Heise, V., Trachtenberg, A. J., & Mackay, C. E. (2013). The forgotten APOE allele: a review of the evidence and suggested mechanisms for the protective effect of APOE ε2. *Neuroscience & Biobehavioral Reviews, 37*(10), 2878–2886.

Trachtenberg, A. J., Filippini, N., & Mackay, C. E. (2012). The effects of APOE-epsilon 4 on the BOLD response. *Neurobiology of Aging, 33*(2), 323–334.

Westlye, E. T., Lundervold, A., Rootwelt, H., Lundervold, A. J., & Westlye, L. T. (2011). Increased hippocampal default mode synchronization during rest in middle-aged and elderly APOE e4 carriers: relationships with memory performance. *Journal of Neuroscience the Official Journal of the Society for Neuroscience, 31*(21), 7775–7783.

Whitwell, J. L., Josephs, K. A., Murray, M. E., Kantarci, K., Przybelski, S., Weigand, S., et al. (2008). MRI correlates of neurofibrillary tangle pathology at autopsy A voxel-based morphometry study. *Neurology, 71*(10), 743–749.

Wu, X., Li, R., Fleisher, A. S., Reiman, E. M., Guan, X., Zhang, Y., et al. (2011). Altered default mode network connectivity in Alzheimer's disease–a resting functional MRI and Bayesian network study. *Human Brain Mapping, 32*(11), 1868–1881.

Yan, H., Zhang, Y., Chen, H., Wang, Y., & Liu, Y. (2013). Altered effective connectivity of the default mode network in resting-state amnestic type mild cognitive impairment. *Journal of the International Neuropsychological Society, 19*(4), 400–409.

Yang, H., Wang, C., Zhang, Y., Xia, L., Feng, Z., Li, D., et al. (2017). Disrupted causal connectivity anchored in the posterior cingulate cortex in amnestic mild cognitive impairment. *Frontiers in Neurology, 8*.

Yuan, B., Xie, C., Shu, H., Liao, W., Wang, Z., Liu, D., et al. (2016). Differential effects of APOE genotypes on the anterior and posterior subnetworks of default mode network in amnestic mild cognitive impairment. *Journal of Alzheimers Disease, 54*(4), 1409.

Zang, Z.-X., Yan, C.-G., Dong, Z.-Y., Huang, J., & Zang, Y.-F. (2012). Granger causality analysis implementation on MATLAB: a graphic user interface toolkit for fMRI data processing. *Journal of Neuroscience Methods, 203*(2), 418–426.

Zhou, Z., Wang, X., Klahr, N. J., Liu, W., Arias, D., Liu, H., et al. (2011). A conditional Granger causality model approach for group analysis in functional magnetic resonance imaging. *Magnetic Resonance Imaging, 29*(3), 418–433.